Modal Inversion SW06 Experiment

Subramaniam D. Rajan
Scientific Solutions, Inc.
99 Perimeter Road
Nashua, NH 03063
Phone: 603-880-3784   e-mail: srajan@scisol.com com

Contract Number: N00014-08-C-0543
http://www.scisol.com

LONG-TERM GOALS

Develop methods for rapid assessment of sediment properties relevant for acoustic propagation in a range-dependent shallow water environment.

OBJECTIVES

Modal dispersion data i.e. mode travel time as a function of frequency have been used in inversion schemes that estimate sediment properties in a range-independent environment. This method has been extended to include range-dependent environment. Simulation studies show that range-dependent sediment properties can be extracted if mode dispersion data are obtained for multiple source/receiver locations [1]. In the Shallow Water 2006 experiment effort was made to collect co-located data sets to perform inversions using both, mode dispersion data and mode eigenvalues. The overlapping data sets will provide a direct means of comparison and evaluation of compressional wave speed profile estimates from mode dispersion data and mode eigenvalues

APPROACH

In shallow water, the acoustic field can be represented as a sum of contributions from a set of propagating modes. It is well known that modal dispersion data contain information about the characteristics of the shallow water wave guide including the acoustic characteristics of the sediment. Inversion scheme that uses the modal dispersion data for estimating sediment acoustic properties in a range independent environment has been described in the literature [2, 3]. This approach has been modified to determine the sediment properties in a range-dependent environment as outlined below.

Using perturbation analysis, the perturbation dt_n in the travel time of mode n at the receiver due to perturbation in the compressional wave speed is given by

$$dt_n = \frac{\partial}{\partial \omega} \int_0^r \int_0^\infty \frac{1}{k_n(s,\omega)} \frac{\omega^2 \Delta c(s,z)}{c_b^3(s,z)\rho_b(s,z)} \left|\phi_n(s,z,\omega)\right|^2 dsdz \qquad (1)$$

Report Documentation Page

Form Approved
OMB No. 0704-0188

1. REPORT DATE **30 SEP 2009**	2. REPORT TYPE **Annual**	3. DATES COVERED **00-00-2009 to 00-00-2009**

4. TITLE AND SUBTITLE
Modal Inversion SW06 Experiment

5a. CONTRACT NUMBER

5b. GRANT NUMBER

5c. PROGRAM ELEMENT NUMBER

6. AUTHOR(S)

5d. PROJECT NUMBER

5e. TASK NUMBER

5f. WORK UNIT NUMBER

7. PERFORMING ORGANIZATION NAME(S) AND ADDRESS(ES)
Scientific Solutions, Inc.,99 Perimeter Road,Nashua,NH,03063

8. PERFORMING ORGANIZATION REPORT NUMBER

9. SPONSORING/MONITORING AGENCY NAME(S) AND ADDRESS(ES)

10. SPONSOR/MONITOR’S ACRONYM(S)

11. SPONSOR/MONITOR’S REPORT NUMBER(S)

12. DISTRIBUTION/AVAILABILITY STATEMENT
Approved for public release; distribution unlimited

13. SUPPLEMENTARY NOTES
Code 1 only

14. ABSTRACT
Develop methods for rapid assessment of sediment properties relevant for acoustic propagation in a range-dependent shallow water environment.

15. SUBJECT TERMS

16. SECURITY CLASSIFICATION OF:			17. LIMITATION OF ABSTRACT	18. NUMBER OF PAGES	19a. NAME OF RESPONSIBLE PERSON
a. REPORT **unclassified**	b. ABSTRACT **unclassified**	c. THIS PAGE **unclassified**	**Same as Report (SAR)**	**9**	

Standard Form 298 (Rev. 8-98)
Prescribed by ANSI Std Z39-18

where ω is the frequency of the acoustic source, $k_n(s, \omega)$ is the eigenvalue of the nth mode, $c_b(s, z)$ is the unperturbed compressional wave speed of the sediment, $\rho_b(s, z)$ is the density of the sediment, $\phi_n(s, z, \omega)$ is the mode function of the nth mode, r is the range to the receiver, $\Delta c(s, z)$ is the perturbation to the compressional wave speed, and s and z represent the range and depth locations. The double integral can be changed into a double sum given below.

$$dt_n = \sum_{p=1}^{P} \sum_{q=1}^{Q} A(s_p, z_q) \Delta c(s_p, z_q) \tag{2}$$

This double sum can be reduced to a matrix equation and the equation solved to determine the quantity $\Delta c(s_p, z_q),\ p = 1, \cdots, P, q = 1, \cdots, Q.$ In converting the integral to a matrix equation we assumed the region is discretized in both range and depth. The argument s_p refers to the pth step in range and z_q refers to the qth step in depth.

In many field experiments it is not possible to synchronize the transmission of the signal with the acquisition of data. In these instances it is not possible to obtain the absolute travel time of the modes. The inverse algorithm indicated above can be modified so as to use mode travel time differences instead of the mode travel time. It has been demonstrated in [1] that this approach also yields satisfactory results.

MODAL INVERSE METHODS EXPERIMENT (MIME)

During 2006 a series of experiments were conducted in the general area of the Hudson Canyon off the coast of New Jersey. A major component of the experiment was Littoral Environment Acoustic Research (LEAR). One aspect of this initiative was Modal Inverse Methods Experiment (MIME). The objective of this part of the experiment was to validate modal inverse methods for the estimation of the sediment acoustic properties. Two approaches are available for estimating the sediment acoustic properties from modal data. In one approach the range-dependent acoustic properties are determined from the evolution of the eigenvalues of trapped modes in the shallow water waveguide. In the second approach, the mode travel times are used estimating the range dependent sediment acoustic properties. The data for evaluating these two methods of geoacoustic inversion in a range-dependent environment were collected during the MIME part of the SW06 experiments.

In order to obtain mode dispersion data broadband signals were transmitted using J-15-3 source. These sources have good response in the band of 50 Hz-600 Hz. Broadband signals (Linear frequency modulated signals) of duration 0.5 seconds and in the band 40 Hz – 290 Hz were transmitted from this source. The signaling scheme at each source location consisted of repeated transmission of the LFM signal. The signals were transmitted every 3 seconds and the total transmission time was approximately 12 minutes.

The broadband transmissions were made on Julian Days 216, 217, and 218. The locations of these transmissions were approximately along two arcs. The data were collected at six receiver locations. Out of these six, five were single hydrophone units (SHRU 49-53) and the sixth was an array (SHARK) which had 48 elements (16 element vertical array and 32 element horizontal array). The location of the broadband transmissions and the location of the receiver units are shown in Fig. 1.

During the course of the experiment, the sound speed structure in the water column was obtained using a CTD chain. In addition to the measuring the sound speed of the water column, the ships sub-bottom profiler was used to determine the bathymetry.

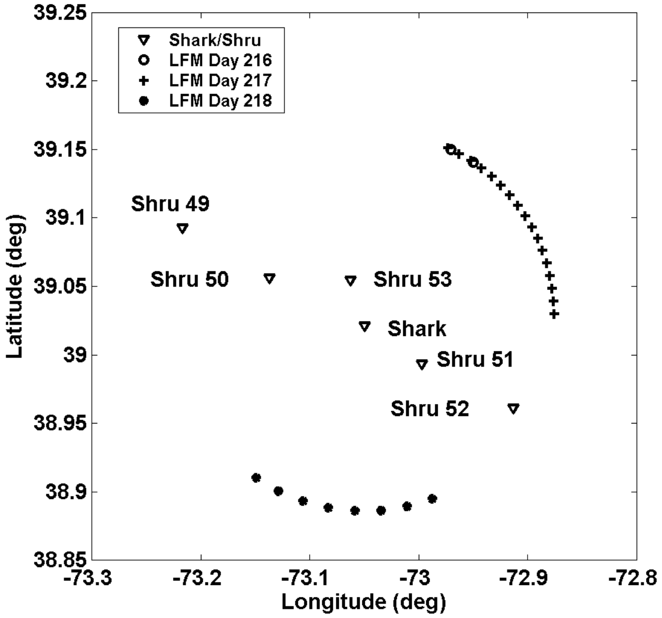

Figure 1. Location of receiver units and locations of broadband transmissions on Days 216, 217 and 218.

RESULTS

A. Estimation of travel time differences

The first step in the estimation of the range-dependent sediment properties is the determination of the travel times of the modes. This is done by the time-frequency analysis of the received signal. In our initial analysis we have concentrated on data collected on Day 217. Though the data for Day 216 had good SNR, it was noted during the analysis that during the time of the transmissions strong internal wave activity was present in the region which affected the propagation of the modes and hence caused errors in the determination of the mode arrival structure.

Mode arrival times are determined by performing time-frequency analysis on the signal acquired at the receiver. Short Time Fourier Transform (STFT) is one of the techniques used to perform time-frequency analysis. Hong et.al [4] proposed a modification of the STFT for dispersive wave analysis. Time-frequency resolution of the STFT is independent of location in the time-frequency plane. The proposed modification to STFT makes it so that tiling in the time-frequency plane is dependent on the dispersive character of the propagating waves. The method is based on the chirplet transform [5] which allows for a generalized time-frequency tiling. This leads to more accurate estimations of modal arrival times from the time-frequency analysis. A brief description of the method is given below.

Consider the STFT as represented in the equation below.

$$STFT(f,\tau) = \int_{-\infty}^{\infty} x(t)g(t-\tau)exp(-i2\pi ft)dt. \tag{3}$$

Here *x (t)* is the signal and *g (t)* is the window function. For a Gaussian window the window function is $g_{(\tau,\zeta,s)}(t) = \frac{1}{\sqrt{s}} g\left(\frac{t-\tau}{s}\right) exp(-i\zeta t)$, where τ and ζ represent the locations in time and frequency, and *s* determines the width of the window. The function *g (t)* for a Gaussian window is $\pi^{-1/4}\, exp(-t^2/2).$ The dispersion based STFT (D-STFT) is defined as [4]

$$\text{D-STFT}(\tau,\zeta) = \int_{-\infty}^{\infty} x(t)\left[\frac{1}{\sqrt{s}} g\left(\frac{t-\tau}{s}\right) * (id)^{-1/2} \exp(-t^2/2d)\right]\exp(-i\zeta t)dt, \tag{4}$$

where * represents the convolution operator and the parameter *d* determines the amount of rotation of the time-frequency block. The parameter *d* is given by the expression

$$d = d(\tau,\zeta) = \frac{\Delta\tau}{\Delta\zeta}. \tag{5}$$

To use the formulation of the dispersion related STFT we need to determine the parameter $d(\tau,\zeta)$. Let the sampling be uniform in both time and frequency, i.e. the location in time and frequency are $\tau_i, i = 1,\cdots,M$ and $\zeta_j, j = 1,\cdots,N$. Let $v(\zeta)$ be the group velocity of any given mode. The distance D traveled by this mode, i.e. the distance between the source and the receiver, at any given time is $D = v(\zeta_j)\tau_i$. Then t_{i-1} and t_{i+1}, the arrival times of neighboring components belonging to ζ_{j-1} and ζ_{j+1}, are given by the expressions $t_{i-1} = \frac{D}{v(\zeta_{j-1})}$ and $t_{i+1} = \frac{D}{v(\zeta_{j+1})}$, so that

$$d(\tau_i,\zeta_j) = \frac{t_{i+1} - t_{i-1}}{\zeta_{j+1} - \zeta_{j-1}} = \frac{\lfloor D/v(\zeta_{j+1}) - D/v(\zeta_{j-1})\rfloor}{\zeta_{j+1} - \zeta_{j-1}}. \tag{6}$$

Because the rotating parameter is linked to the mode dispersion in the time-frequency plane the resulting tiling is close to the dispersion. In order to use this method we need to know the dispersion characteristics of the propagating wave. Typically, we do not know this *a priori*. A starting model with a given dispersion relation is assumed. The starting model is iterated on until the dispersion relation of the model matches that of the data. It has been shown in [1] that D-STFT performs better that STFT. In view of this, analysis of the data was repeated using D-STFT during the current report period.

The spectrum of the signal received at the single hydrophone receiver unit (SHRU 51) is shown in the left panel of Fig. 2(a). The spectrum shows multiple pings of the broadband signal. Each of these pings are then subjected to time-frequency analysis. The time-frequncy plot for one set of pings transmitted during Day 217 is shown in the middle panel of Fig. 2(b). The full line in this figure shows the modes 1, 2, and 3 as obtained by D-STFT. The right panel (Fig. 2(c)) shows the mode travel time difference between modes 1 and 2 obtained using D-STFT and STFT for one of the pings. The figure shows that the differences between these two estimates is large at the lower frequencies. This is attributable to the more accurate estimate of mode arrival time by D-STFT at the lower frequencies where the SNR is not high..

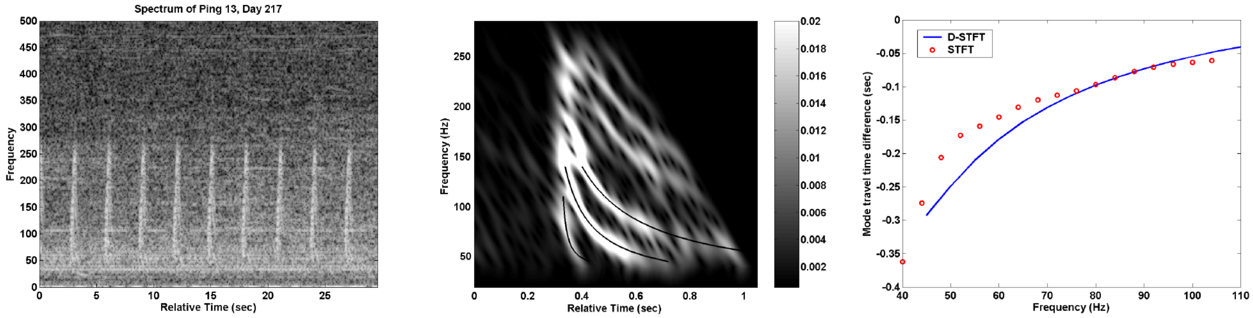

(a) **(b)** **(c)**

Figure 2. (a) Shows the spectrum of the received signal, (b) reflects the time frequency analysis of the ping, and (c) compares the modal travel time difference obtained bt D-STFT and STFT.

B. Geo-acoustic Inversion

In order to determine the range-dependent compressional wave speed in the region between the source and receivers, the region was divided into six regions. Four shots locations and three receiver locations were used in the analysis giving a total of twelve source receiver combinations. The shot locations were Pings 13, 14, 15, and 16 of Day 217 and receiver locations were that of the shark array, SHRU 51 and SHRU 53. The division of the regions into six regions together with the location of the pings and the receivers are shown in the left panel of Fig. 3(a).

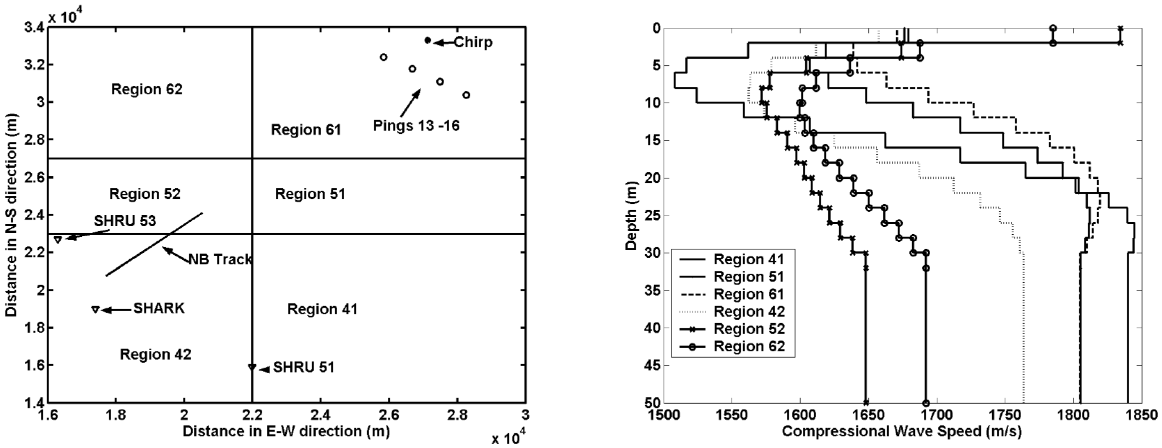

(a) **(b)**

Figure 3. (a) shows the six regions for which the compressional wave speed profiles were determined. The division into the six regions was loosely based on the surficial compressional wave speed which is also shown in the figure; (b) shows the compressional wave speed profiles of the six regions estimated by inversion.

In performing the inversion, the sediment was assumed to be horizontally stratified. A total number of 16 layers with each layer thickness of 2 m was assumed. The only unknown was the compressional wave speed in the layer. The layers were terminated by a half space. The density in the layer was assumed to be 1.6 gm/cc and in the half space 1.8 gm/cc. The attenuation in the sediment layers were ignored.

The mode travel time differences obtained by performing time-frequency analysis with D-STFT were the input data for the range-dependent inversions The inversions were performed in stages. In the first step, using data received at SHRU 51, the wave speed profile in Region 41, 51, and 61 were obtained. Then using data from SHRU 53, the profiles for Regions 52 and 62 were obtained. Finally using data from SHARK array the profile for Region 42 was determined.

The compressional wave speed profiles for the six regions are shown in the right panel of Fig. 3(b). It is noted that the profiles have similar general structure.

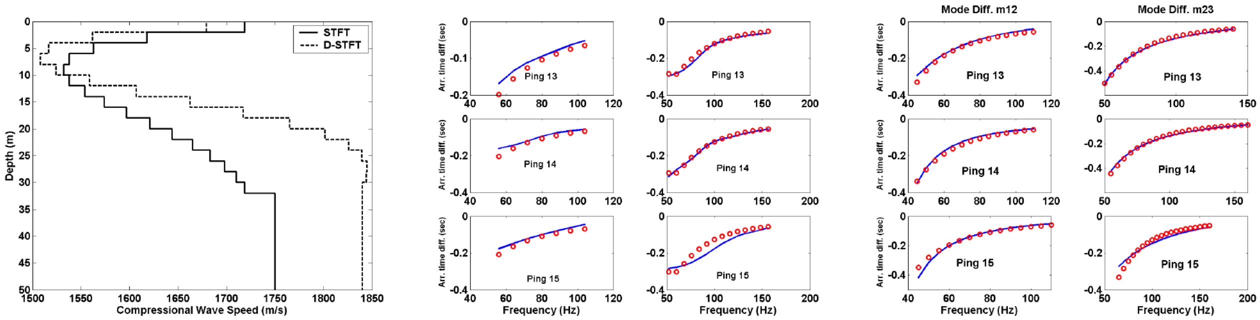

(a) **(b)** **(c)**

Figure 4. (a) shows the compressional wave speed profile for Region 41 obtained with data from analysis based on STFT and D-STF; (b) shows the agreement between the mode travel time differences determined from experiment data using STFT and the mode travel time difference predicted by the model obtained using this data; (c) shows similar comparison for model obtainedusing D-STFT data.

We had indicated that the time-frequency analysis using D-STFT was done in view of its better performance. In the left panel of Fig. 4(a) we compare the compressional wave speed profiles for one of the regions obtained by using data estimated by both STFT and D-STFT. We note that the maximum deviation between the profiles is at deeper depths. This is consistent with the maximum difference in mode travel time differences occuring at lower frequencies as mode functions for the lower frequencies penetrate to deeper sediment depths. The middle and right panels of Fig. 4(b)(c) the mode travel time differences obtained from experiment data and the model predicted values of mode travel time differences are shown in respect of Pings 13, 14, and 15 to the receiver unit SHRU 51. It is seen that the agreement between the experimentally determined mode travel time differences and that predicted by the model is better in respect of model obtained from D-STFT data.

C. Validation of the results

The compressional wave speed profiles for the six regions obtained by inverting the mode travel time differences have been evaluated and found to be consistent with models obtained by other investigators. This is fully described in [1].

D. Analysis of data of Day 218

On Day 218 transmissions were made from eight locations. Of these eight only two transmissions (Pings 7 and 8) has suffcient signal to noise ratio to enable time-frequency analysis of the data. In respect of other transmissions the signal was corrupted by transmissions from other sources. The locations of the transmissions are shown in the left panel of Fig. 5 (a). The signal at all the receiver units (SHRU 49 – SHRU 53) and SHARK array have sufficient SNR for the estimation of travel time through time-frequency analysis. The right panel of Fig. 5(b) shows the additional areas for which it will be possible to determine the compressional wave speed profile using the travel time data estimated from the data collected on Day 218.

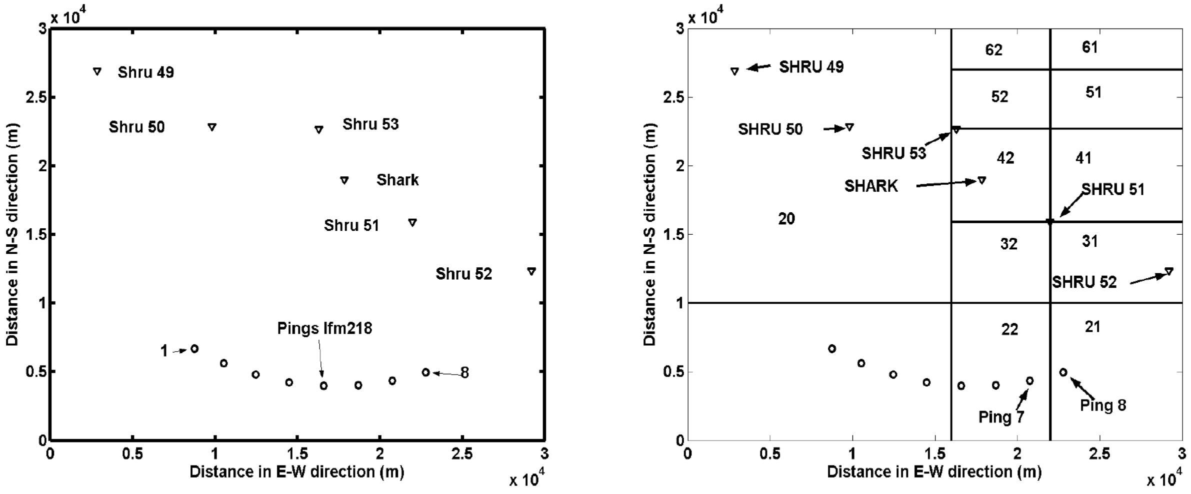

(a) (b)

Figure 5. (a) shows the disposition of the receiver units and the transmissions on Day 218; (b) shows the division of the region between the shot locations and the receiver units in to 11 range independent sections. Of these 11, the compressional wave speed profiles for six regions were determined using Day 217 data. Day 218 data will be used to estimate the compressional wave speed profiles in the remaining 5 regions (20,21,22,31,32).

The bathymetry at the locations of the transmissions (Pings 7 and 8) is approximately 96 m where as the ocean depth at the receiver locations are around 82-84 m. It is also seen that this depth change over a dsitance of 5 km. The applicability of adiabatic approximation to this case is being investigated in order to ascertain if the procedure outlined earlier for estimating range-dependent sediment properties is applicable. This work is currently in progress.

IMPACT/APPLICATIONS

The data collected during this experiment will enable validation of the proposed method for estimating range-dependent sediment compressional wave speed from modal dispersion data. Using a distributed set of receivers and a moving broadband source it will be possible to estimate the compressional wave speed profiles over a wide area. This will therefore be a useful tool for rapid environment assessment.

RELATED PROJECTS

A number of investigators were involved in the SW06 experiment. The analysis of their data will also lead to estimation of sediment properties. A direct comparison between the different inversion methods can therefore be done. Extensive environmental measurements taken during the experiment will help in assessing the impact of variability in water column characteristics.

REFERENCES

1. S. D. Rajan and K.M. Becker, “Inversions for range-dependent sediment compressional wave speed profiles from mode dispersion data,” Submitted to *IEEE Journal of Oceanic Engineering*.

2. S. D. Rajan, J. F. Lynch, and G. V. Frisk, "Perturbative inversion methods for obtaining bottom geoacoustic parameters in shallow water,” *Journal of the Acoustical Society of America*, 82(3), 998-1017, 1987.

3. J. F. Lynch, S. D. Rajan, and G. V. Frisk, "A comparison of broadband and narrowband inversions for bottom geoacoustic properties at a site near Corpus Christi, Texas," *Journal of the Acoustical Society of America*, 89(2), 648-655, 1991.

4. Jin-Chul Hong, Kyung Ho Sung, and Yoon Young Kim,” Dispersion based short-time Fourier transform applied to dispersive wave analysis,” *Journal of the Acoustical Society of America*, 117, 2949-2960, 2005

5. S. Mann and S. Haykin, “Chirplet transform. Physical considerations.”, *IEEE Transactions of Signal Processing*, 43, 2745-2761, 1995.